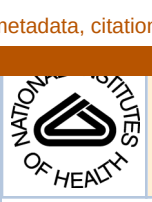

Published in final edited form as:
Hepatology. 2011 August ; 54(2): 664–674. doi:10.1002/hep.24393.

Genetic Ablation or Chemical Inhibition of Phosphatidylcholine Transfer Protein Attenuates Diet-Induced Hepatic Glucose Production

Ekaterina Y. Shishova[1,*], **Janis M. Stoll**[1,*], **Baran A. Ersoy**[1], **Sudeep Shrestha**[1], **Erez F. Scapa**[2], **Yingxia Li**[1], **Michele W. Niepel**[1], **Ya Su**[3], **Linda A. Jelicks**[4], **Gregory L. Stahl**[5], **Marcie Glicksman**[6], **Roger Gutierrez-Juarez**[3], **Gregory D Cuny**[6], and **David E. Cohen**[1]

[1]Department of Medicine, Brigham and Women's Hospital, Harvard Medical School, Boston, Massachusetts, 02115, USA

[2]Gastroenterology Department, Sourasky Medical Center, Tel-Aviv, Israel

[3]Department of Medicine, Albert Einstein College of Medicine, Bronx, New York, 10461, USA

[4]Department of Physiology and Biophysics, Albert Einstein College of Medicine, Bronx, New York, 10461, USA

[5]Department of Anesthesiology, Perioperative and Pain Medicine, Brigham and Women's Hospital, Harvard Medical School, Boston, Massachusetts, 02115, USA

[6]Department of Neurology, Brigham and Women's Hospital, Harvard Medical School, Boston, Massachusetts, 02115, USA

Abstract

Phosphatidylcholine transfer protein (PC-TP, synonym StARD2) is a highly specific intracellular lipid binding protein that is enriched in liver. Coding region polymorphisms in both humans and mice appear to confer protection against measures of insulin resistance. The current study was designed to test the hypotheses that *Pctp*$^{-/-}$ mice are protected against diet-induced increases in hepatic glucose production and that small molecule inhibition of PC-TP recapitulates this phenotype. *Pctp*$^{-/-}$ and wild type mice were subjected to high fat feeding, and rates of hepatic glucose production and glucose clearance were quantified by hyperinsulinemic euglycemic clamp studies and pyruvate tolerance tests. These studies revealed that high fat diet-induced increases in hepatic glucose production were markedly attenuated in *Pctp*$^{-/-}$ mice. Small molecule inhibitors of PC-TP were synthesized and their potencies, as well as mechanism of inhibition, were characterized *in vitro*. An optimized inhibitor was administered to high fat fed mice and used to explore effects on insulin signaling in cell culture systems. Small molecule inhibitors bound PC-TP, displaced phosphatidylcholines from the lipid binding site and increased the thermal stability of the protein. Administration of the optimized inhibitor to wild type mice attenuated hepatic glucose production associated with high fat feeding, but had no activity in *Pctp*$^{-/-}$ mice. Indicative of a mechanism for reducing glucose intolerance that is distinct from commonly utilized insulin-sensitizing agents, the inhibitor promoted insulin-independent phosphorylation of key insulin signaling molecules. These findings suggest PC-TP inhibition as a novel therapeutic strategy in the management of hepatic insulin resistance.

Contact Information, David E. Cohen, Brigham and Women's Hospital, 77 Avenue Louis Pasteur, HIM 941, Boston, MA 02115. Phone: (617) 525-5090; Fax: (617) 525-5100; dcohen@partners.org.
*These authors contributed equally.

Keywords

obesity; insulin resistance; diabetes; StARD2; lipid binding protein

Phosphatidylcholine transfer protein (PC-TP) is a soluble highly specific lipid binding protein with accentuated expression in the liver (1). PC-TP was identified, purified and named based on its capacity to catalyze the intermembrane exchange of phosphatidylcholines *in vitro* (2). According to its characteristic lipid binding pocket that accommodates a single phosphatidylcholine molecule (3), PC-TP has been designated StARD2 within the steroidogenic acute regulatory protein–related transfer (START) domain superfamily (3, 4). Specificity for binding phosphatidylcholines is conferred by a uniquely structured phosphorylcholine head group binding site within the lipid binding pocket of PC-TP (3). Interestingly, evidence for a biological role for PC-TP in lipid transport *in vivo* is generally lacking (5), and we have instead reported the unanticipated finding that PC-TP regulates glucose metabolism (6): Livers of chow fed *Pctp*$^{-/-}$ mice exhibit increased insulin sensitivity, as evidenced by profound decreases in hepatic glucose production under hyperinsulinemic euglycemic clamp conditions (6). Although the molecular mechanism is not fully understood, PC-TP may control hepatic glucose homeostasis in response to variations in the fatty acyl composition of membrane phospholipids (5).

Type 2 diabetes is characterized by excess hepatic glucose production due to insulin resistance, commonly in the setting of obesity (7). As evidenced by coding region polymorphisms in both humans and mice, PC-TP may play a pathogenic role. A Glu10Ala substitution in human subjects in the Quebec Family Study was correlated with a three-fold lower risk of the atherogenic small dense LDL phenotype (8), which is commonly associated with insulin resistance (9). In New Zealand Obese (NZO) mice, an Arg120His substitution in PC-TP appeared to play a protective role against the development of obesity-associated type 2 diabetes (5, 10). The current study was designed to provide a direct test of whether *Pctp*$^{-/-}$ mice are resistant to high fat diet-induced increases in hepatic glucose metabolism and whether small molecule inhibition of PC-TP would recapitulate this phenotype.

Materials and Methods

Mice, diet and treatments

Pctp$^{-/-}$ and wild type control mice 7 generations backcrossed into FVB/NJ genetic background (11) were housed in a standard 12 h alternate light/dark cycle facility, and fed a standard rodent diet 5001 (LabDiets, St. Louis, MO) with free access to drinking water. Protocols for animal use and euthanasia were approved by the institutional committees of the Harvard Medical School and the Albert Einstein College of Medicine. Experiments were conducted using male mice. Starting at 4 – 5 w of age, mice were fed a high fat diet (60 % kcal; D12492; Research Diets, New Brunswick, NJ) for periods ranging from 8 to 18 w prior to commencing experiments. Mice were weighed weekly and rates of food consumption were calculated per mouse from the weight of food withdrawn by all of the mice in the cage each week. Prior to selected experiments, mice were anesthetized by i.p. injection of ketamine (87 mg/kg b.w.) plus xylazine (13 mg/kg b.w.) (Webster Veterinary, Sterling, MA). In experiments designed to test the influence of PC-TP inhibition on glucose homeostasis, administration of compound A1 (see Supporting Information - Materials and Methods for synthesis and assays of microsomal stability and pharmacokinetics) or vehicle was initiated concurrently with the high fat diet. Compound A1 was prepared to a final concentration of 0.6 mg/ml in 4% DMSO and 96% of 6% hydroxypropyl-β-cyclodextrin (Sigma Aldrich, St. Louis, MO) solution in sterile water. Mice were injected i.p. 5 d per w

with 3 mg/kg compound A1 or the equivalent volume of vehicle (5 μl/g). For all experiments, mice were sacrificed after an overnight fast.

Analytical techniques

Plasma non-esterified fatty acids (NEFA), triglyceride, cholesterol and phospholipid concentrations were determined using reagent kits from Wako (Richmond, VA), Sigma Aldrich and Roche Diagnostics (Indianapolis, IN), respectively. Blood glucose was determined using a OneTouch Ultra glucose monitor (LifeScan, Milpitas, CA). Hepatic concentrations of triglycerides and cholesterol were measured enzymatically following hepatic lipid extraction (12). Plasma insulin, leptin and adiponectin were determined by ELISA as a service of the Joslin Diabetes and Endocrinology Research Center Specialized Assay Core (NIH 5P30 DK36836, Joslin Diabetes Center, Boston, MA). Plasma activities of alanine aminotransferase (ALT) and concentrations of bilirubin were determined using standard assays by Charles River Research Animal Diagnostic Services (Wilmington, MA). To assess protein expression, liver tissue or cell lysates were homogenized in RIPA buffer supplemented with protease and phosphatase inhibitors (Roche Diagnostics). Lysates were rotated slowly at 4 °C for 30 min and then centrifuged at 12,000 × g for 10 min to remove cellular debris. Proteins were fractionated by SDS-PAGE and subjected to immunoblot analysis. An anti-PC-TP rabbit polyclonal antibody was as described (13). Antibodies against pAkt(S473)/total Akt, pS6K(T389)/total S6K, pGSK3β(S9), pAMPK(T172)/total AMPK were from Cell Signaling Technology (Beverly, MA). An antibody against total GSK3β was from BD Transduction Laboratories (Woburn, MA), and an antibody against β-actin was from Sigma Aldrich. Detection was by enhanced chemiluminescence using a Western Lightning chemiluminescence reagent (PerkinElmer, Waltham, MA). For histologic analysis, sections of liver were fixed in 10% formalin. Samples were processed, sectioned and stained for hematoxylin and eosin as a service of the Dana-Farber/Harvard Cancer Center Rodent Histopathology Core (supported in part by an NCI Cancer Center Support Grant NIH 5P30 CA06516).

Magnetic resonance imaging of body fat

Images of mice were acquired with a GE/Omega 9.4 Tesla vertical wide-bore spectrometer operating at a ^{1}H frequency of 400 MHz and equipped with 50-mm shielded gradients (General Electric, Fremont, CA) and a 40-mm ^{1}H imaging coil (RF Sensors, New York, NY). The following parameters were used to obtain transverse and sagittal images: echo time, 30 msec; field of view, 51.2 mm; number of averages, 2; slice thickness, 3 mm; gap 0.5 mm, repetition time, 0.4 sec; matrix size, 128 × 256 (interpolated to 256 × 256). Water images were acquired with the water peak on resonance, fat images were acquired with the lipid CH_2 peak on resonance (14). Imaging data were analyzed using MATLAB-based software (The MathWorks, Natick, MA). Spectroscopy studies were conducted prior to imaging using the same coil and a routine pulse-acquire sequence (4 signal averages, 5 sec delay between scans). The areas under the fat and water peaks were integrated using the spectrometer software and were used to calculate the %fat/water and %fat mass.

Pyruvate and glucose tolerance tests

Pyruvate and glucose tolerance tests were performed after an overnight fast (15–17). Plasma glucose was measured at baseline. This was followed by i.p. injection of 2 mg/g b.w. of sodium pyruvate (0.4 g/ml in sterile PBS) for pyruvate tolerance tests or 1 mg/g b.w. D-glucose (20% wt/vol) for glucose tolerance tests. Blood glucose concentrations were measured periodically for up to 180 min. For experiments in which both were performed, mice were allowed to recover for 1 w in between pyruvate and glucose tolerance tests.

Hyperinsulinemic euglycemic clamp studies

Studies were performed in conscious, unrestrained mice fitted with intravenous catheters (18). Briefly, food was removed 5 h prior to commencing the studies, and infusions lasted for 90 min. Mice received a constant infusion of HPLC purified insulin (3.6 mU/min/kg b.w.) and [^{3}H-3]-glucose (0.1 μCi/min; PerkinElmer). A glucose solution (10% wt/vol) was infused at a variable rate so that plasma glucose concentration was constant at 8 mM throughout the experiment. Plasma glucose concentrations and specific activities were used to determine rates of glucose uptake and hepatic glucose production (6).

Structure-activity relationships of small molecule inhibitors and mechanism of PC-TP inhibition

As described in Supporting Information - Materials and Methods, recombinant PC-TP, StARD7 and StARD10 were purified, and small molecule inhibitors were synthesized and used in assays of phosphatidylcholine transfer activity, PC-TP-inhibitor binding by surface plasmon resonance, displacement of pyrene-labeled phosphatidylcholine (Pyr-PC), thermal stability using ThermoFluor and PPARγ activation.

Phosphorylation of signaling proteins in cultured cells

Frozen primary human hepatocytes (CellzDirect/Invitrogen, Carlsbad, CA) were thawed using cryopreserved hepatocyte recovery medium, then plated in serum containing plating media for 6 h to allow cells to adhere. After overnight starvation in serum free medium, compounds A1 or B1 dissolved in DMSO was added (0.1% final concentration of DMSO) for 60 min. Negative controls included no addition and 0.1% DMSO. The positive control included 0.1% DMSO plus insulin (50 nM) for 30 min. Compound A1 was also tested in human embryonic kidney (HEK) 293E cells (19). HEK 293E were maintained in DMEM supplemented with 10% fetal calf serum and 1% penicillin-streptomycin and then starved overnight. Cells were then exposed to compound A1 for 60 min.

Statistics

Data are reported as means ± SEM. Differences between groups were analyzed using a two-tailed unpaired Student's *t*-test.

Results

Attenuation of diet-induced hepatic glucose production in high fat fed *Pctp*$^{-/-}$ mice

In mice fed a high fat diet, the lack of PC-TP expression did not influence growth or food consumption (Supporting Fig. 1A) and obesity was evidenced by body weights that exceeded chow fed counterparts (6) by up to 40%. After 8 w, fasting plasma glucose concentrations (Fig. 1A) were similar to those previously reported for chow fed mice (6) and were similarly decreased in *Pctp*$^{-/-}$ mice. The high fat diet for 12 w was sufficient in wild type mice to elevate plasma glucose concentrations, which did not rise in *Pctp*$^{-/-}$ mice until 18 w. As a result, the absence of PC-TP expression was associated with 25%, 46%, and 17% reductions in fasting plasma glucose concentrations at 8, 12, and 18 w of high fat feeding, respectively. Hyperinsulinemic euglycemic clamp studies performed after 18 w revealed a 3.6 fold increase in glucose infusion rate in *Pctp*$^{-/-}$ mice (Fig. 1B). Whereas the rate of glucose uptake was unchanged, hepatic glucose production was decreased by 46%. In order validate an alternative, more facile procedure to determine rates of hepatic glucose production, mice fed the high fat diet for 12 w were subjected to pyruvate tolerance tests (16). Reduced plasma glucose concentrations were observed in *Pctp*$^{-/-}$ mice during the course of the pyruvate tolerance tests (Fig. 1C), such that the mean values for area under the curve (AUC) were reduced 32% compared with wild type mice.

Percentages of body fat, as well as other metrics of body and plasma compositions were measured after 12 w on the high fat diet. In contrast to our previous findings (6), the percentages of body fat in high fat fed mice did not differ between the two genotypes (inset to Supporting Fig. 1A). Moreover, liver and epididymal fat pad weights were similar (Table 1) and both macro- and micro-vesicular hepatic steatosis were equally present (Supporting Fig. 2). High fat fed *Pctp*$^{-/-}$ mice did not exhibit changes in leptin or adiponectin concentrations or in plasma or hepatic concentrations of insulin, NEFA, triglycerides, cholesterol and phospholipids (Table 1).

Identification of an optimized small molecule inhibitor of PC-TP

In a high-throughput screening of 114,752 compounds, we previously identified 6 distinct small molecule inhibitors of the phosphatidylcholine transfer activity of PC-TP (20). To select an optimized molecule for a therapeutic trial in mice, we synthesized structural analogs around the two most potent inhibitors identified in the screen, A1 and B1 (Fig. 2). Structure-activity analyses using a fluorescence quench assay (Supporting Fig. 3) revealed molecular features that influence the IC_{50} values (Fig. 2). For the A series, at least one halogen group on the terminal ring at R_1 was essential for inhibition. The addition of a methyl substituent to the aryl amide at R_3 reduced inhibition more than 30-fold. Finally, the two methyl substituents at R_5 were essential for inhibitory activity. For the B series, essential features for inhibition included a sulfur atom at position X, a Ph on the α-carbon of the amide at R_2, as well as the nature of substituents on the terminal ring, particularly 2,3-dichloro at R_4. Additionally, the introduction of methyl on the amide nitrogen at R_3 eliminated inhibition. StARD10 activity was inhibited by selected compounds, but less effectively (Supporting Fig. 3B), with the IC_{50} values (Fig. 2) ranging from 1.5 – 10 fold greater than for PC-TP. StARD7 was only modestly inhibited by compounds A1 and B1 (IC_{50} ~70 μM) and more weakly inhibited by other compounds at higher IC_{50} values that could not be quantified under conditions of the assay.

Compound A1 binds PC-TP, displaces phosphatidylcholine and increases thermal stability

We used surface plasmon resonance to demonstrate binding of representative inhibitors directly to PC-TP with K_D values in the micromolar range (Fig. 3A). Compound A10, which demonstrated no inhibitory activity (Fig. 2) did not bind PC-TP. Because the parent compounds from each series (i.e. A1 and B1) exhibited both the lowest IC_{50} values and greatest specificity for PC-TP, these were tested for *in vitro* microsomal stability in order to determine their potential utilities *in vivo*. This revealed a 6.5-fold greater metabolic stability of compound A1 (compound A1, half-life ($t_{1/2}$) = 230 min and intrinsic clearance (Cl_{int}) = 6.0 μL/min/mg protein; compound B1, $t_{½}$ = 35.6 min and Cl_{int} = 39 μL/min/mg protein). Based on this result, we selected compound A1 (LDN-193188) for additional characterization. In a fluorescence competition assay, compound A1 displaced a fluorescent phosphatidylcholine from the lipid binding pocket of PC-TP (Fig. 3B). The K_{rel} value for compound A1 was 20% of the K_{rel} for phosphatidylcholine (inset to Fig. 3B). Finally, we demonstrated that compound A1 increased the thermal stability of PC-TP (Fig. 3C): The T_m of PC-TP, which was markedly increased when PC-TP was bound by phosphatidylcholine, was further increased when bound by compound A1 (inset to Fig. 3C).

Compound A1 attenuates diet-induced hepatic glucose production in wild type mice

Based upon a pharmacokinetic analysis, which revealed a maximum plasma concentration (C_{max}) = 54 μM, time to maximum concentration (t_{max}) = 0.5 h and $t_{1/2}$ = 19.4 h following a single 3 mg/kg i.p. dose of compound A1, we designed a dosing schedule in which 3 mg/kg of inhibitor or the equivalent volume of vehicle was administered i.p. daily for 5 d per w for 12 w. Mice administered the inhibitor exhibited similar weight gain and food consumption as vehicle-treated mice (Supporting Figs. 1B and 1C), although neither group gained as

much weight as high fat fed mice that were not subjected to i.p. injection (Supporting Fig. 1A).

Treatment with compound A1 led to a 31% reduction in fasting plasma glucose concentrations (mg/dl) in wild type mice, but did not significantly affect *Pctp*$^{-/-}$ mice (Table 1). The inhibitor improved glucose tolerance tests for wild type mice (Fig. 4A), as evidenced by separation of the response curves and a 20% reduction in AUC compared with vehicle-treated controls. *Pctp*$^{-/-}$ mice did not respond to inhibitor treatment (Fig. 4B). Consistent with decreased hepatic glucose production, compound A1 also improved the pyruvate tolerance tests of wild type but not *Pctp*$^{-/-}$ mice (Figs. 4C and D), with separation of response curves and a 20% reduction in AUC for wild type mice, which did not achieve statistical significance. For both glucose and pyruvate tolerance tests, the similar peak glucose concentrations and AUC values in wild type mice treated with compound A1 and in *Pctp*$^{-/-}$ mice treated with either compound A1 or vehicle suggests that PC-TP was completely inhibited by compound A1.

Treatment of mice with compound A1 did not alter plasma concentrations of insulin or NEFA (Table 1). Although body composition was not measured directly in these mice, there were no changes in epididymal fat pad weights or plasma concentrations of leptin and adiponectin. In livers of wild type mice treated with compound A1, we observed increases in triglyceride and cholesterol concentrations together with non-significant increases in plasma triglyceride and cholesterol concentrations. Livers of mice treated with either compound A1 or vehicle exhibited microvesicular steatosis, but did not show histologic evidence of toxicity or inflammation (Supporting Fig. 2). Treatment with compound A1 was not associated with ALT elevations (Supporting Fig. 4A), and plasma bilirubin concentrations tended to decline in both genotypes (Supporting Fig. 4B).

Compound A1 activates insulin signaling

Fig. 5A shows insulin-independent increases in the phosphorylation of Akt, p70 ribosomal S6 kinase (S6K) and glycogen synthase kinase 3β (GSK3β) following exposure of cultured primary human hepatocytes or HEK 293E cells to concentrations of compound A1 achieved *in vivo*. This suggested that compound A1 augments the intrinsic cellular response to insulin signaling due to specific inhibition of PC-TP. Similar effects of compound B1 in primary human hepatocytes (Supporting Fig. 5A) support this assertion, as does increased basal phosphorylation of Akt and S6K in livers of fasted wild type but not *Pctp*$^{-/-}$ mice treated with compound A1 (Fig. 5B and Supporting Fig. 5B). The absence of changes in PC-TP expression in cultured cells or in livers of inhibitor treated wild type mice (Fig. 5A and Supporting Fig. 5) indicates that small molecule inhibition does not reduce PC-TP expression or accelerate its degradation. Finally, we tested compounds A1 and B1 for activation of PPARγ (Supporting Fig. 6), but neither compound exhibited this activity.

Discussion

Our interest in PC-TP as a therapeutic target was motivated by the unexpected initial finding of increased hepatic insulin sensitivity in chow fed *Pctp*$^{-/-}$ mice (6). These mice exhibited reduced fasting plasma glucose concentrations and profound decreases in hepatic glucose production under conditions of a hyperinsulinemic-euglycemic clamp. In addition to increased Akt phosphorylation in cultured primary hepatocytes that lacked PC-TP expression, an increased percentage of body fat in *Pctp*$^{-/-}$ mice was associated elevated plasma concentrations of both leptin and adiponectin. These findings suggested two potential mechanisms for increased hepatic insulin sensitivity; intrinsic sensitization of hepatocytes to insulin and adipokine-mediated sensitization of the liver to insulin action. The current study confirms and extends our observations in chow fed mice by demonstrating

that *Pctp*$^{-/-}$ mice are resistant to diet-induced glucose intolerance, but not to obesity. The high fat diet eliminated genotype-dependent differences in body composition and adipokines, as well as plasma and hepatic concentrations of NEFA, triglycerides and cholesterol. Therefore, the persistent decrease in hepatic glucose production was most likely attributable to intrinsic sensitivity of the liver to insulin action in the absence of PC-TP expression. When taken together with genetic evidence that PC-TP polymorphisms are protective against insulin resistance in humans (8) and mice (10), these findings prompted us to examine whether pharmacological inhibition of PC-TP would recapitulate the same effects and serve as proof-of-concept for a novel therapeutic modality.

In order to identify an optimized small molecule inhibitor for a therapeutic trial in mice, we subjected the two most potent compounds identified in a small molecule screen (20) to systematic structure-function analyses. These identified molecular features required for inhibition, but did not ultimately generate compounds with *in vitro* potencies beyond those observed for the parent molecules (i.e. compounds A1 and B1). To further characterize the inhibitors, we tested their specificity against other mammalian proteins that exhibit phosphatidylcholine transfer activity *in vitro* (5). We selected two closely related START domain proteins (21). StARD10 is overexpressed in some primary human breast cancers (22), and like PC-TP, it binds and transfers phosphatidylcholines *in vitro* (23). StARD10 activity was inhibited by compound A1, but less effectively. StARD7 is a highly expressed protein in a choriocarcinoma cell line (24) and exhibits phosphatidylcholine transfer activity (25). It was only modestly inhibited by compounds A1 and B1, although precise IC_{50} values for these weakly active compounds could not be quantified under conditions of the assay. These findings suggest that small molecule inhibition was at least relatively selective for the structural characteristics of PC-TP.

An important unresolved question from the initial high-throughput screen (20) was the mechanism of inhibition. The *in vitro* activity of PC-TP in the fluorescence quench assay reflects a multistep process (20): The protein must first associate with a donor small unilamellar vesicle, exchange a phosphatidylcholine molecule, dissociate from the vesicle, associate with an acceptor small unilamellar vesicle, again exchange a phosphatidylcholine and then dissociate. Therefore, it was possible that the small molecule inhibitors might not bind directly to PC-TP, but may have instead inserted into the membrane bilayer and disrupted membrane association of the protein. Because such a mechanism would likely reduce the therapeutic potential of an inhibitor *in vivo*, we explored whether the compounds bound directly to PC-TP. Surface plasmon resonance, which is a sensitive biophysical technique for the measurement of ligand protein interactions (26), revealed that inhibitors of PC-TP bound the protein with K_D values that were in good agreement with respective IC_{50} values. In further support of an inhibitory mechanism that involved direct binding to the protein, compound A1 displaced a fluorescent phosphatidylcholine analog from the PC-TP lipid binding pocket, displaying similar relative affinity for PC-TP as natural phosphatidylcholines. Compound A1 also increased the thermal stability of PC-TP, providing additional independent evidence for inhibitor-protein binding.

Because of its favorable metabolic and pharmacokinetic characteristics, we selected compound A1 for *in vivo* testing. Consistent with a PC-TP-dependent mechanism of glucose regulation, the administration of this compound to high fat fed mice led to significant reductions in fasting plasma glucose concentrations and improved glucose tolerance tests for wild type, but not *Pctp*$^{-/-}$ mice. Due to prohibitive logistical issues, we were unable to perform hyperinsulinemic euglycemic clamp studies to determine whether inhibitor treatment reduced hepatic glucose production. We therefore used pyruvate tolerance tests as a more facile surrogate measure of hepatic glucose production. In a pyruvate tolerance test, the gluconeogenic substrate pyruvate is converted to glucose by the liver and exported into

plasma (16). Having validated this approach against hyperinsulinemic euglycemic clamp studies using untreated high fat fed mice, pyruvate tolerance tests were utilized to demonstrate a PC-TP-dependent reduction in hepatic glucose production by compound A1.

Inhibitor treatment of wild type mice was not associated with differences in plasma concentrations NEFA, leptin and adiponectin, or in other lipid-related parameters that might influence insulin sensitivity (27). These findings suggested that inhibitor-mediated improvements in glucose homeostasis were attributable to the activity of compound A1 in the liver. This possibility was tested in primary human hepatocytes and HEK 293 cells, both of which exhibited robust expression of PC-TP. Exposure of cells to PC-TP inhibitors resulted in dose-dependent, but insulin-independent activation of Akt, p70-S6K and GSK3β, which are key effectors of insulin signaling (28). The relevance of these findings *in vivo* was evidenced by increased basal levels of pAkt and p70-S6K in wild type, but not *Pctp*$^{-/-}$ mice treated with compound A1. The possibility that compound A1 enhances insulin signaling is consistent with our recent observations in HEK 293 cells following siRNA-mediated knockdown of PC-TP (Ersoy et al., Hepatology 2010;52:591, abstract).

Metformin and thiazolidinediones are commonly utilized insulin sensitizing agents to manage type 2 diabetes. The absence of consistent increases in phosphorylation of AMP-activated protein kinase (AMPK) suggests a distinct activity of compound A1 from metformin (29, 30). Compound A1 also failed to activate PPARγ, arguing against a mechanism in common with thiazolidinediones (7, 31). In addition, the absence of ALT or bilirubin elevations and lack of histologic evidence of liver damage or inflammation indicated that chronic treatment of mice with compound A1 was not associated with hepatotoxicity. The reductions in plasma bilirubin concentrations were observed in both wild type and *Pctp*$^{-/-}$ mice, suggesting an additional off-target effect of compound A1. Possible explanations include the induction of bilirubin metabolism or biliary secretion. Because the objective in measuring plasma concentrations was to evaluate potential hepatoxicity of compound A1, we have not yet pursued a mechanistic explanation in the current study.

An important limitation of this study is that treatment with both compound A1 and vehicle reduced weight gain together with fasting plasma glucose concentrations and degrees of glucose intolerance in both genotypes when compared with untreated mice. Although likely attributable to the frequency of i.p. injections performed during the 12 w treatment period, it is possible that the vehicle, which contained 2-hydroxypropyl-β-cyclodextrin, did exert metabolic effects. This could explain the noticeable difference in distribution of hepatic lipids in treated mice, which exhibited microvesicular hepatic steatosis despite similar tissue lipid concentrations as untreated mice in which we observed both macro- and microvesicular distributions of hepatic fat. Appreciating that the administration of 2-hydroxypropyl-β-cyclodextrin to mice can increase intracellular cholesterol transport (32), further study will be required to ascertain the specific influence of the vehicle on hepatic lipid distribution. We also noted tendencies toward increased hepatic and plasma concentrations of triglycerides and cholesterol in both wild type and *Pctp*$^{-/-}$ mice treated with compound A1. The occurrence of these changes independent of PC-TP expression is suggestive of an off-target effect of the small molecule, the mechanism for which is not yet understood.

In summary, this study has served as proof of principle that genetic or chemical targeting of PC-TP in a mouse model can attenuate diet-induced glucose intolerance by sensitizing the liver to insulin action and reducing hepatic glucose production. If small molecule inhibitors of PC-TP prove to be capable of treating established type 2 diabetes, they could represent a novel approach to the management of this common disorder. Moreover, these compounds

should be of value in efforts to dissect the molecular mechanisms by which PC-TP regulates hepatic glucose metabolism.

Supplementary Material

Refer to Web version on PubMed Central for supplementary material.

List of Abbreviations

ALT	alanine aminotransferase
AMPK	AMP-activated protein kinase
AUC	area under the curve
Cl_{int}	intrinsic clearance
C_{max}	maximum plasma concentration
DHPE	Lissamine rhodamine B 1,2-dihexadecanoyl-sn-glycero-3-phosphoethanolamine, triethylammonium salt
F	fluorescence intensity
GSK3β	glycogen synthase kinase 3β
HEK	human embryonic kidney
K_{rel}	relative affinity
NEFA	non-esterified fatty acids
NZO	New Zealand Obese
NBD-PC	2-[12-(7-Nitrobenz-2-oxa-1,3-diazol-4-yl)amino]dodecanoyl-1-hexadecanoyl-sn-glycero-3 phosphocholine
PA	phosphatidic acid
TCNQ	7,7,8,8-tetracyanoquinodimethane
PC-TP	phosphatidylcholine transfer protein
PE	phosphatidylethanolamine
PPARγ	peroxisome proliferator-activated receptor γ
Pyr-PC	1-Hexadecanoyl-2-(1-pyrenedecanoyl)-sn-glycero-3-phosphocholine
S6K	p70 ribosomal S6 kinase
SM	sphingomyelin
START	steroidogenic acute regulatory protein-related transfer
T_m	melting temperature
t_{max}	time to maximum concentration

Acknowledgments

Financial Support

This work was supported by National Institutes of Health grants to D.E.C. (DK56626 and DK48873) and R.G.-J. (DK45024), by Partners Healthcare and by an unrestricted gift from Johnson and Johnson. This work was also conducted with support from the Harvard Catalyst The Harvard Clinical and Translational Science Center (N.I.H. Award #UL1 RR 025758 and financial contributions from Harvard University and its affiliated academic health

care centers) and the Harvard Digestive Diseases Center (P30 DK34854). J.M.S. was supported by a National Institutes of Health T32 grant (DK07477). E.F.S. was the recipient of an American Liver Foundation Irwin M. Arias Postdoctoral Research Fellowship Award.

We are grateful to Dr. Ji-Feng Liu at Aberjona Laboratories (Beverly, MA) for synthesizing inhibitor analogs and to Dr. Xin Teng, Brigham and Women's Hospital, for preparing sufficient amounts of compound A1 (LDN-193188) for *in vivo* studies. The authors thank Drs. Jorge Plutzky and Gabriela Orasanu for assistance with the experiment to test activation of PPARγ, Drs. Ross Stein, David Brooks and David Silver for helpful discussions and Mr. James Macdiarmid for editorial assistance with the manuscript.

References

1. Kanno K, Wu MK, Scapa EF, Roderick SL, Cohen DE. Structure and function of phosphatidylcholine transfer protein (PC-TP)/StarD2. Biochim. Biophys. Acta. 2007; 1771:654–662. [PubMed: 17499021]
2. Wirtz KW. Phospholipid transfer proteins. Annu. Rev. Biochem. 1991; 60:73–99. [PubMed: 1883207]
3. Roderick SL, Chan WW, Agate DS, Olsen LR, Vetting MW, Rajashankar KR, Cohen DE. Structure of human phosphatidylcholine transfer protein in complex with its ligand. Nature Struct Biol. 2002; 9:507–511. [PubMed: 12055623]
4. Ponting CP, Aravind L. START: a lipid-binding domain in StAR, HD-ZIP and signalling proteins. Trends Biochem. Sci. 1999; 24:130–132. [PubMed: 10322415]
5. Kang HW, Wei J, Cohen DE. PC-TP/StARD2: Of membranes and metabolism. Trends Endocrinol. Metab. 2010; 21:449–456. [PubMed: 20338778]
6. Scapa EF, Pocai A, Wu MK, Gutierrez-Juarez R, Glenz L, Kanno K, Li H, et al. Regulation of energy substrate utilization and hepatic insulin sensitivity by phosphatidylcholine transfer protein/StarD2. FASEB J. 2008; 22:2579–2590. [PubMed: 18347010]
7. Samuel VT, Petersen KF, Shulman GI. Lipid-induced insulin resistance: unravelling the mechanism. Lancet. 2010; 375:2267–2277. [PubMed: 20609972]
8. Dolley G, Berthier MT, Lamarche B, Despres JP, Bouchard C, Perusse L, Vohl MC. Influences of the phosphatidylcholine transfer protein gene variants on the LDL peak particle size. Atherosclerosis. 2007; 195:297–302. [PubMed: 17266964]
9. Chahil TJ, Ginsberg HN. Diabetic dyslipidemia. Endocrinol. Metab. Clin. North Am. 2006; 35:491–510. [PubMed: 16959582]
10. Pan HJ, Agate DS, King BL, Wu MK, Roderick SL, Leiter EH, Cohen DE. A polymorphism in New Zealand inbred mouse strains that inactivates phosphatidylcholine transfer protein. FEBS Lett. 2006; 580:5953–5958. [PubMed: 17046758]
11. Wu MK, Hyogo H, Yadav S, Novikoff PM, Cohen DE. Impaired response of biliary lipid secretion to a lithogenic diet in phosphatidylcholine transfer protein-deficient mice. J. Lipid Res. 2005; 46:422–431. [PubMed: 15576839]
12. Hyogo H, Roy S, Paigen B, Cohen DE. Leptin promotes biliary cholesterol elimination during weight loss in ob/ob mice by regulating the enterohepatic circulation of bile salts. J. Biol. Chem. 2002; 277:34117–34124. [PubMed: 12114517]
13. Shoda J, Oda K, Suzuki H, Sugiyama Y, Ito K, Cohen DE, Feng L, et al. Etiologic significance of defects in cholesterol, phospholipid, and bile acid metabolism in the liver of patients with intrahepatic calculi. Hepatology. 2001; 33:1194–1205. [PubMed: 11343249]
14. Barac-Nieto M, Gupta RK. Use of proton MR spectroscopy and MR imaging to assess obesity. J. Magn. Reson. Imaging. 1996; 6:235–238. [PubMed: 8851434]
15. Ilany J, Bilan PJ, Kapur S, Caldwell JS, Patti ME, Marette A, Kahn CR. Overexpression of Rad in muscle worsens diet-induced insulin resistance and glucose intolerance and lowers plasma triglyceride level. Proc. Natl. Acad. Sci. U.S.A. 2006; 103:4481–4486.
16. Rodgers JT, Puigserver P. Fasting-dependent glucose and lipid metabolic response through hepatic sirtuin 1. Proc. Natl. Acad. Sci. U.S.A. 2007; 104:12861–12866. [PubMed: 17646659]
17. Ayala JE, Samuel VT, Morton GJ, Obici S, Croniger CM, Shulman GI, Wasserman DH. Standard operating procedures for describing and performing metabolic tests of glucose homeostasis in mice. Dis Model Mech. 2010; 3:525–534. [PubMed: 20713647]

18. Okamoto H, Obici S, Accili D, Rossetti L. Restoration of liver insulin signaling in Insr knockout mice fails to normalize hepatic insulin action. J. Clin. Invest. 2005; 115:1314–1322. [PubMed: 15864351]
19. Kanno K, Wu MK, Agate DA, Fanelli BK, Wagle N, Scapa EF, Ukomadu C, et al. Interacting proteins dictate function of the minimal START domain phosphatidylcholine transfer protein/StarD2. J. Biol. Chem. 2007; 282:30728–30736. [PubMed: 17704541]
20. Wagle N, Xian J, Shishova EY, Wei J, Glicksman MA, Cuny GD, Stein RL, et al. Small-molecule inhibitors of phosphatidylcholine transfer protein/StarD2 identified by high-throughput screening. Anal. Biochem. 2008; 383:85–92. [PubMed: 18762160]
21. Soccio RE, Breslow JL. StAR-related lipid transfer (START) proteins: mediators of intracellular lipid metabolism. J. Biol. Chem. 2003; 278:22183–22186. [PubMed: 12724317]
22. Olayioye M, Hoffmann P, Pomorski T, Armes J, Simpson R, Kemp B, Lindeman G, et al. The phosphoprotein StarD10 is overexpressed in breast cancer and cooperates with ErbB receptors in cellular transformation. Cancer Res. 2004; 64:3538–3544. [PubMed: 15150109]
23. Olayioye MA, Vehring S, Muller P, Herrmann A, Schiller J, Thiele C, Lindeman GJ, et al. StarD10, a START domain protein overexpressed in breast cancer, functions as a phospholipid transfer protein. J. Biol. Chem. 2005; 280:27436–27442. [PubMed: 15911624]
24. Angeletti S, Rena V, Nores R, Fretes R, Panzetta-Dutari GM, Genti-Raimondi S. Expression and localization of StarD7 in trophoblast cells. Placenta. 2008; 29:396–404. [PubMed: 18378304]
25. Horibata Y, Sugimoto H. StarD7 mediates the intracellular trafficking of phosphatidylcholine to mitochondria. J. Biol. Chem. 2010; 285:7358–7365. [PubMed: 20042613]
26. Montalto MC, Collard CD, Buras JA, Reenstra WR, McClaine R, Gies DR, Rother RP, et al. A keratin peptide inhibits mannose-binding lectin. J. Immunol. 2001; 166:4148–4153. [PubMed: 11238665]
27. Biddinger SB, Kahn CR. From mice to men: insights into the insulin resistance syndromes. Annu Rev Physiol. 2006; 68:123–158. [PubMed: 16460269]
28. Taguchi A, White MF. Insulin-like signaling, nutrient homeostasis, and life span. Annu Rev Physiol. 2008; 70:191–212. [PubMed: 17988211]
29. Miller RA, Birnbaum MJ. An energetic tale of AMPK-independent effects of metformin. J. Clin. Invest. 2010; 120:2267–2270. [PubMed: 20577046]
30. Zhou G, Myers R, Li Y, Chen Y, Shen X, Fenyk-Melody J, Wu M, et al. Role of AMP-activated protein kinase in mechanism of metformin action. J. Clin. Invest. 2001; 108:1167–1174. [PubMed: 11602624]
31. Mayerson AB, Hundal RS, Dufour S, Lebon V, Befroy D, Cline GW, Enocksson S, et al. The effects of rosiglitazone on insulin sensitivity, lipolysis, and hepatic and skeletal muscle triglyceride content in patients with type 2 diabetes. Diabetes. 2002; 51:797–802. [PubMed: 11872682]
32. Liu B, Turley SD, Burns DK, Miller AM, Repa JJ, Dietschy JM, et al. Reversal of defective lysosomal transport in NPC disease ameliorates liver dysfunction and neurodegeneration in the npc1−/− mouse. Proc Natl Acad Sci USA. 2009; 106:2377–2382. [PubMed: 19171898]
33. Van Paridon PA, Gadella TWJ, Somerharju PJ, Wirtz KWA. On the relationship between the dual specificity of the bovine brain phosphatidylinositol transfer protein and membrane phosphatidylinositol levels. Biochim. Biophys. Acta. 1987; 903:68–77. [PubMed: 3651458]

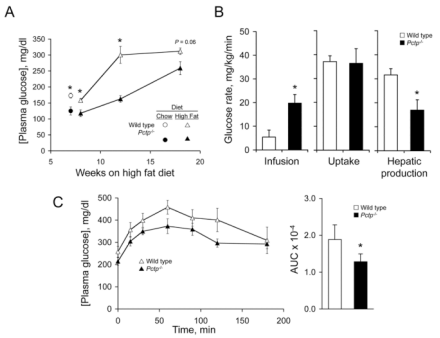

Figure 1. *Pctp*$^{-/-}$ mice are resistant to diet-induced glucose intolerance

(A) Reduced fasting plasma glucose concentrations in mice lacking PC-TP. Wild type (n = 6 – 10) and *Pctp*$^{-/-}$ (n = 8 – 10) mice were fed a high fat (60% kcal) diet for up to 18 w. Values for chow fed wild type and *Pctp*$^{-/-}$ mice of similar age to mice fed high fat for 8 w are replotted from reference (6). (B) Decreased hepatic glucose production in *Pctp*$^{-/-}$ mice. Values determined by hyperinsulinemic euglycemic clamp studies for wild type mice (n = 6) and *Pctp*$^{-/-}$ mice (n = 8) fed the high fat diet for 18 w. (C) Pyruvate tolerance tests reflect changes in hepatic glucose production. Wild type (n = 4) and *Pctp*$^{-/-}$ (n = 5) mice fed high fat diet for 12 w were subjected to pyruvate tolerance tests. The barplot gives mean AUC values. *$P < 0.05$ versus wild type mice.

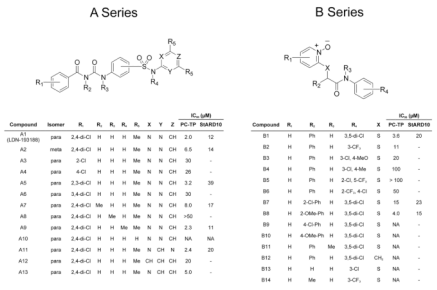

Compound	Isomer	R_1	R_2	R_3	R_4	R_5	X	Y	Z	IC_{50} (μM) PC-TP	IC_{50} (μM) StARD10
A1 (LDN-193189)	para	2,4-di-Cl	H	H	H	Me	N	N	CH	2.0	12
A2	meta	2,4-di-Cl	H	H	H	Me	N	N	CH	6.5	14
A3	para	2-Cl	H	H	H	Me	N	N	CH	30	-
A4	para	4-Cl	H	H	H	Me	N	N	CH	26	-
A5	para	2,3-di-Cl	H	H	H	Me	N	N	CH	3.2	39
A6	para	3,4-di-Cl	H	H	H	Me	N	N	CH	30	-
A7	para	2,4-di-Cl	Me	H	H	Me	N	N	CH	8.0	17
A8	para	2,4-di-Cl	H	Me	H	Me	N	N	CH	>50	-
A9	para	2,4-di-Cl	H	H	Me	Me	N	N	CH	2.3	11
A10	para	2,4-di-Cl	H	H	H	H	N	N	CH	NA	NA
A11	para	2,4-di-Cl	H	H	H	Me	N	CH	N	2.4	20
A12	para	2,4-di-Cl	H	H	H	Me	CH	CH	CH	20	-
A13	para	2,4-di-Cl	H	H	H	Me	N	CH	CH	5.0	-

Compound	R_1	R_2	R_3	R_4	X	IC_{50} (μM) PC-TP	IC_{50} (μM) StARD10
B1	H	Ph	H	3,5-di-Cl	S	3.6	20
B2	H	Ph	H	3-CF_3	S	11	-
B3	H	Ph	H	3-Cl, 4-MeO	S	20	-
B4	H	Ph	H	3-Cl, 4-Me	S	100	-
B5	H	Ph	H	2-Cl, 5-CF_3	S	> 100	-
B6	H	Ph	H	2-CF_3, 4-Cl	S	50	-
B7	H	2-Cl-Ph	H	3,5-di-Cl	S	15	23
B8	H	2-OMe-Ph	H	3,5-di-Cl	S	4.0	15
B9	H	4-Cl-Ph	H	3,5-di-Cl	S	NA	-
B10	H	4-OMe-Ph	H	3,5-di-Cl	S	NA	-
B11	H	Ph	Me	3,5-di-Cl	S	NA	-
B12	H	Ph	H	3,5-di-Cl	CH_2	NA	-
B13	H	H	H	3-Cl	S	NA	-
B14	H	Me	H	3-CF_3	S	NA	-

Figure 2. Structure-activity relationships of PC-TP inhibitors

Structures and inhibitory characteristics of small molecules derived from compounds A1 and B1. “NA” denotes that a compound exhibited no activity, and “-” denotes that no measurement was performed. Syntheses of small molecular inhibitors are illustrated in Supporting Information.

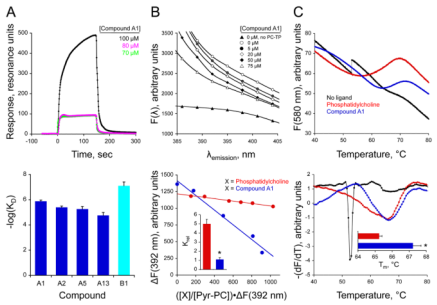

Figure 3. Compound A1 binds PC-TP, displaces phosphatidylcholine and increases thermal stability

(A) Binding of compound A1 to PC-TP as assessed by surface plasmon resonance. Upper panel: Compound A1 (50 – 100 μM) was injected for 150 s to allow binding and then dissociation from PC-TP bound to a CM5 chip. Representative sensograms are shown overlaid and zeroed on the y-axis to the average baseline before injection. The injection start time for each sample was set to zero on the x-axis. Lower panel: Selected inhibitors were analyzed by surface plasmon resonance. Rate constants of association (k_a) and dissociation (k_d) were determined by non-linear least squares analysis of the sensogram data (SigmaPlot, Systat Software, San Jose, CA) and used to calculate equilibrium dissociation constants, $K_D = k_d/k_a$. (B) Displacement of phosphatidylcholine from PC-TP by compound A1. Upper panel: Emission scans of Pyr-PC in the absence of PC–TP or with PC–TP plus compound A1. Lower panel: Relative affinity constants, K_{rel}, were determined according to the equation (33) $\Delta F(392\ nM) = -1/K_{rel}\cdot([X]/[Pyr– PC])\cdot\Delta F(392\ nM) + \Delta F_{max}$ for X = phosphatidylcholine or compound A1 by linear regression of ΔF plotted against the product of ΔF(392 nM) and the molar ratio [X]/[Pyr-PC]. The inset bar plot displays values of K_{rel} (n = 3 – 4 determinations) for phosphatidylcholine and compound A1. **P* = 0.0001. (C) Stabilization of PC-TP by compound A1 using a thermal shift (ThermoFluor) assay. Fluorescence intensity (upper panel) and first derivative, dF/dT of the melting curves (lower panel) for PC–TP, PC–TP plus phosphatidylcholine and PC–TP with compound A1. Values of T_m were determined using LightCycler Protein Melting software (Roche), which identified T_m as minimum values of −dF/dT when plotted as functions of temperature. The inset bar plot shows the comparison of the T_m values (n = 3 determinations) of PC–TP plus phosphatidylcholine, and PC–TP plus compound A1. **P* = 0.02.

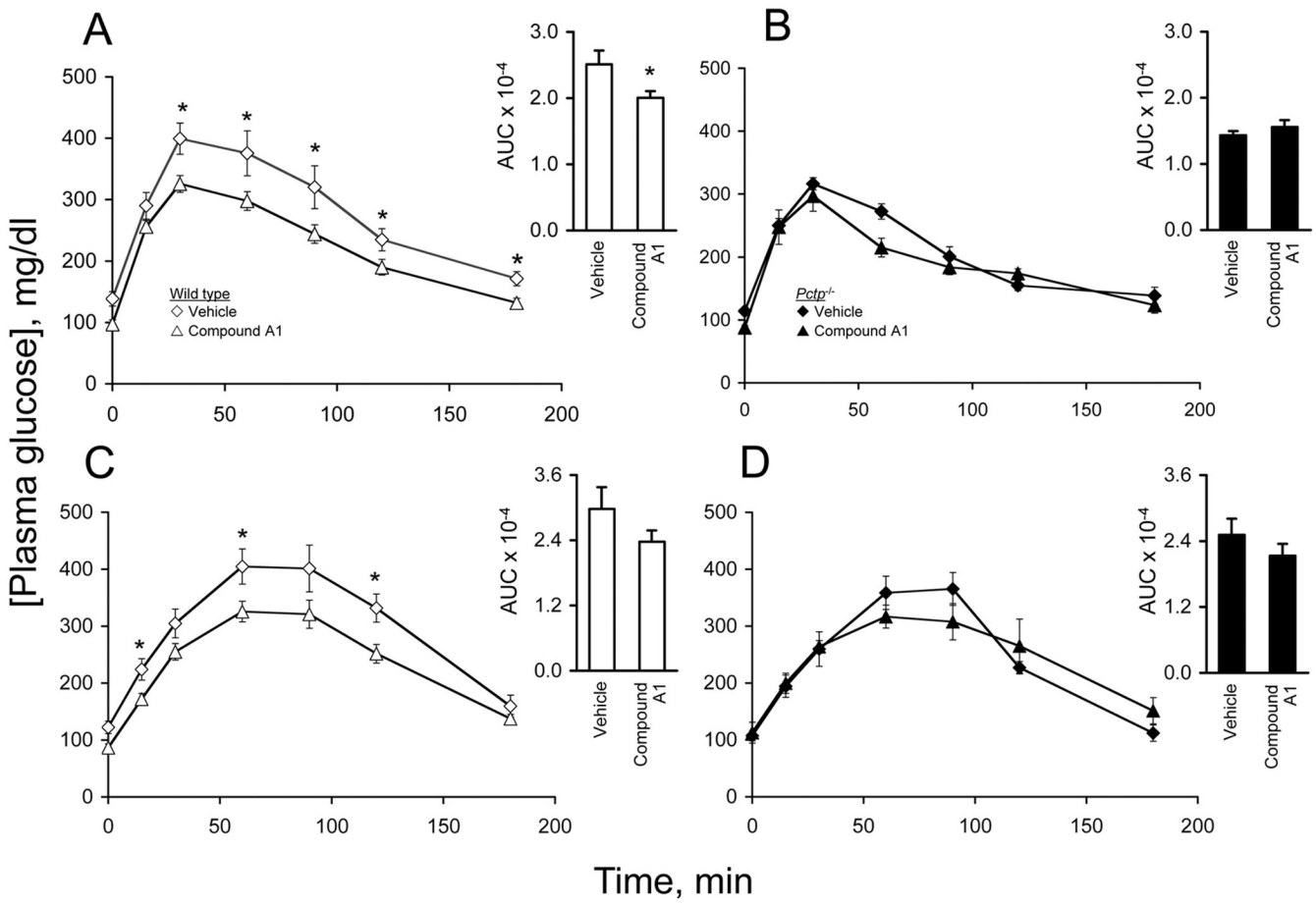

Figure 4. Compound A1 improves glucose homeostasis in high fat fed wild type but not *Pctp*$^{-/-}$ mice

Improved glucose and pyruvate tolerance tests in wild type mice treated with compound A1. High fat fed wild type mice and *Pctp*$^{-/-}$ mice were injected i.p. 5 d per w with 3 mg/kg of compound A1 for 12 w. Mice were subjected to glucose tolerance tests (A: wild type - vehicle n = 4, compound A1 n = 8; B: *Pctp*$^{-/-}$ - vehicle n = 3, compound A1 n = 4) and pyruvate tolerance tests (C: wild type - vehicle n = 4, compound A1 n = 7; D: *Pctp*$^{-/-}$ - vehicle n = 3, compound A1 n = 3). The inset bar plots provide AUC values for wild type mice and *Pctp*$^{-/-}$ mice. *$P < 0.05$ versus vehicle treatment.

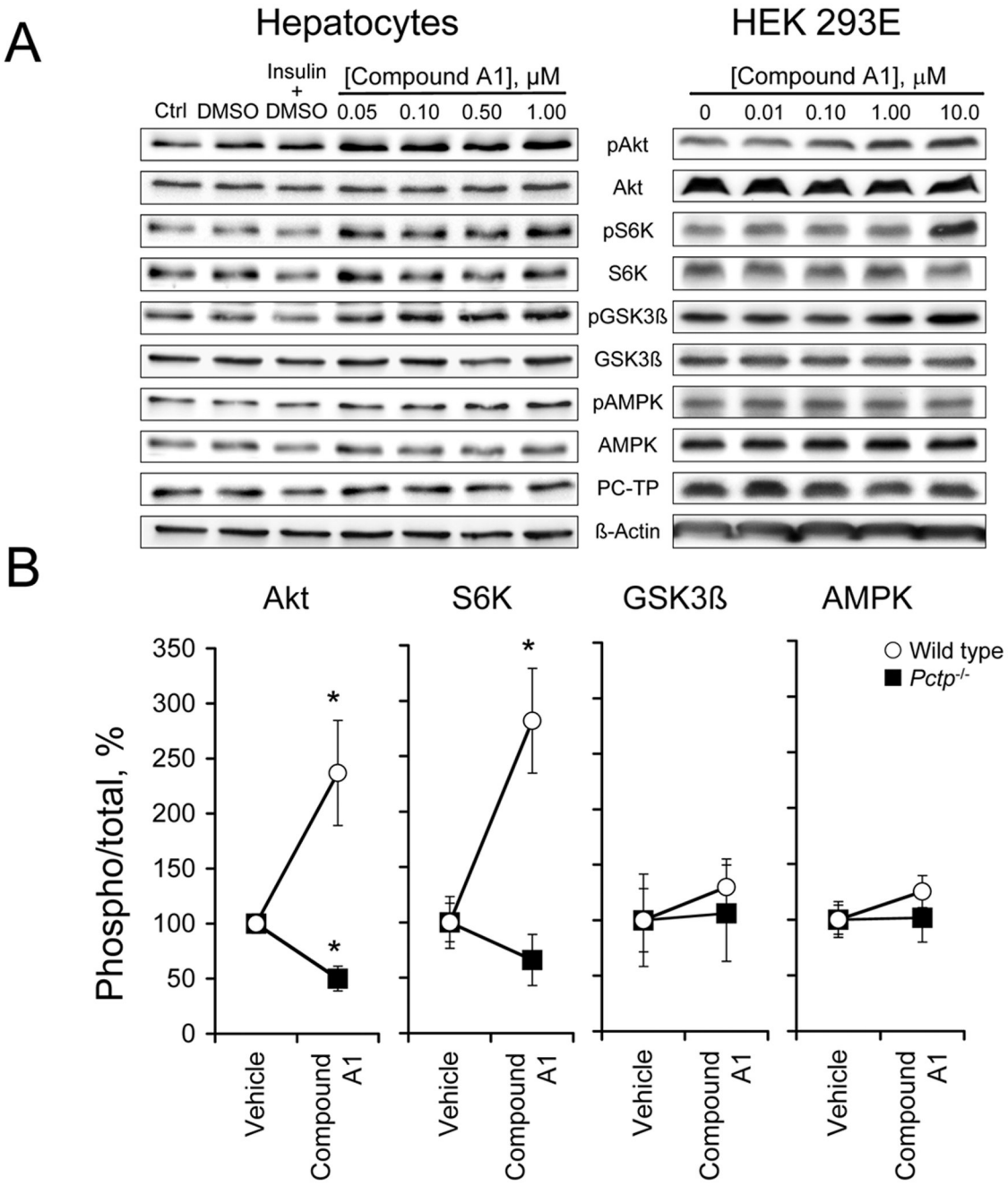

Figure 5. Compound A1 enhances insulin signaling

(A) Compound A1 increases phosphorylation of selected mediators of insulin signaling in cultured cells. Human hepatocytes (left panel) and HEK 293E cells (right panel) were serum starved overnight, then treated with compound A1 for 1 h and harvested for immunoblot analyses. Results are representative of 2 experiments for human hepatocytes and 3 experiments for HEK 293E cells. (B) Compound A1 increases phosphorylation of Akt and S6K in livers of wild type mice. Homogenates of liver samples from mice fasted overnight were subjected to immunoblotting and bands (Supporting Fig. 5B) were quantified by densitometry. *$P < 0.05$ versus vehicle treatment.

Table 1

Characteristics of fasting wild type and *Pctp*$^{-/-}$ mice following 12 w of high fat feeding [a]

	Wild type [b]	*Pctp*$^{-/-}$	Wild type [c]	Wild type	*Pctp*$^{-/-}$[c]	*Pctp*$^{-/-}$
	(n = 7)	(n = 10)	(n = 8)	(n = 5)	(n = 4)	(n = 3)
Treatment	---	---	A1	Vehicle	A1	Vehicle
Weight						
Body (g)	40.4 (1.3)	40.0 (0.7)	27.5 (0.6)	29.1 (0.4)	26.2 (0.6)	29.1 (1.3)
Liver (g)	1.48 (0.07)	1.65 (0.10)	1.25 (0.05)	1.28 (0.06)	1.13 (0.06)	1.37 (0.03)
Epididymal fat pad (g)	1.26 (0.09)	0.95 (0.11)	1.02 (0.07)	0.94 (0.07)	0.85 (0.12)	1.00 (0.1)
Plasma concentration						
Glucose (mg/dl)	300.6 (26.5)	162.5 (10.2) [d]	92.7 (4.4)	133.4 (9.9) [e]	97.0 (8.5)	110.7 (5.7)
Insulin (ng/ml)	0.23 (0.03)	0.24 (0.02)	0.15 (0.01)	0.15 (0.01)	0.14 (0.01)	0.14 (0.02)
Leptin (ng/ml)	64.6 (8.7)	59.5 (7.2)	4.1 (0.8)	3.4 (0.8)	3 (0.9)	5.4 (1.9)
Adiponectin (μg/ml) [f]	14.6 (3.9)	8.6 (1.3)	9.8 (0.6)	8.9 (0.5)	8.7 (0.6)	8.5 (0.5)
NEFA (μM)	310 (40)	428 (61)	417 (42)	511 (75)	400 (49)	358 (117)
Triglycerides (mg/dl)	60.7 (4.4)	70.5 (7.6)	30.6 (5.1)	21.9 (6.1)	34.2 (5.2)	11.8 (2) [e]
Cholesterol (mg/dl)	140 (10)	168 (16)	110 (11)	86 (12)	117 (8)	87 (13)
Phospholipids (mg/dl) [g]	187.6 (12)	191.8 (15)	117.5 (29)	120 (27)	118.7 (37)	97 (44)
Hepatic concentration						
Triglycerides (mg/g)	97.2 (8.4)	92.8 (7.6)	98.3 (6.9)	59.9 (13.4) [e]	62.7 (12.6)	50.2 (5.0)
Cholesterol (mg/g)	2.2 (0.1)	2.2 (0.1)	3.0 (0.1)	2.5 (0.2) [e]	2.8 (0.3)	2.6 (0.3)

[a] Mice were fed a high fat (60% kcal) diet for 12 w prior to sacrifice under fasting conditions. Mice treated with compound A1 or vehicle were injected i.p. 5 d per w for 12 w, starting when the high fat diet was initiated. Data are presented as mean (SEM).

[b] Values for wild type and *Pctp*$^{-/-}$ mice were compared using two-tailed unpaired Student's *t*-test.

[c] Values for mice treated with compound A1 and vehicle were compared using two-tailed unpaired Student's *t*-test.

[d] $P < 0.05$ versus wild type mice.

[e] $P < 0.05$ versus compound A1 treated mice.

[f] For untreated mice: wild type, n = 6; *Pctp*$^{-/-}$, n = 8.

[g] The phospholipid assay utilized choline oxidase, which detects plasma phosphatidylcholines and sphingomyelins. In a prior study (Wu and Cohen. Am J Physiol 2005;289:G1067-74), we have demonstrated that lack of PC-TP expression in mice did not influence plasma phospholipid concentration or composition, which principally comprises phosphatidylcholines (~60%) with lesser proportions of sphingomyelins (~15%).